Geotechnical Aspects of Underground Construction in Soft Ground – Viggiani (ed)
© 2012 Taylor & Francis Group, London, ISBN 978-0-415-68367-8

Effect of pressurized grouting on anchor behavior in residual soils

Tae-Sub Kim
Shinwha Soil Tech. Co., Ltd., Seoul, Korea

Bo-Kyoung Sim
Hyundai Eng. and Const. Co., Ltd., Seoul, Korea

Jong-Sun Kim
Korea University Seoul, Korea

Seok-Won Lee
Konkok University Seoul, Korea

In-Mo Lee
Korea University Seoul, Korea

ABSTRACT: The purpose of this study is to figure out the effect of pressurized grouting on diameter enlargement and pullout resistance of the compression ground anchor installed in decomposed residual soils. The laboratory chamber tests were carried out for 3-types of soils which are abundant in Korean peninsula. These tests simulate the real construction process of a ground anchor with pressurized grouting. Experimental results showed that grout permeation effect into the ground through porous media has to be taken into account when estimating the anchor diameter, if the permeability of the ground is larger than 10^{-3} cm/sec. A series of in-situ anchor pullout tests was executed in 3 different sites which represent 3 types of residual soils used in laboratory chamber tests. Results of in-situ tests showed that the effect of the pressurized grouting is more prominent in a softer ground with smaller SPT-N value. Based on experimental results, a new equation to estimate the pullout resistance as a function of the SPT-N value was proposed which might be applicable to decomposed residual soils.

1 INSTRUCTION

Various types of ground anchors are frequently used in earth-retaining structures such as a retaining wall, a slope, and tieback during excavation. In designing the compression ground anchor, the pullout resistance is a key parameter which varies subject to the installation method, soil dilation, roughness of anchor surface, shear strength of the soil, group effect, grout injection method, and so on.

Regarding the effect of pressurized grouting on pullout resistance in a ground anchor, Hobst & Zajic (1983) carried out laboratory pullout tests on the ground anchor and showed a significant increase in pullout resistance due to the pressurized grouting. Kleyner et al. (1993) discussed the effect of grout pressure on the capacity of bore-injected piles and anchors. Recently, Yin et al. (2008) investigated the increase of pullout resistance in a soil nailing system caused by pressurized grouting through the laboratory pullout tests. Even though some previous studies have applied the cavity expansion theory to the analysis on the enlargement of the anchor body diameter due to pressurized grouting, the penetration (permeation) characteristics of the cement grout have not been properly taken into consideration in their studies.

This paper evaluates the effect of pressurized grouting on pullout resistance of a compression ground anchor according to the soil types by performing both the pilot-scale laboratory chamber tests and field tests. Not only the cavity expansion theory but also the grout penetration theory are adopted in this study and are compared with experimental test results to investigate the effect of pressurized grouting on the enlargement of the anchor body diameter. Based on field ground anchor pullout tests, a new equation to estimate the pullout resistance proposed, which might be applicable to decomposed residual soils.

2 THEORIES UTILIZED FOR PRESSURIZED GROUTING

2.1 *Cavity expansion theory*

In this study, the cavity expansion theory based on the equations of elasto-plastic analysis by Yu & Houlsby (1991) is modified to be more suitable for analyzing the pressurized grouting.

The pressurized ground anchor is generally constructed by a continuous process of drilling and grout injection into a borehole under pressure. During drilling, the plastic zone is developed around a circular borehole leading to inward displacement in the stress state of $\sigma_r < \sigma_\theta$, where σ_r and σ_θ are stresses in the radial and tangential directions, respectively. This stress condition can be defined as an active loading condition. When pressurized grouting is performed, σ_r increases while σ_θ decreases in the plastic zone. Hence, the stress state moves towards an isotropic stress state, $\sigma_r = \sigma_\theta$, through a stress reversal, and then perhaps moves to another yield state where $\sigma_r > \sigma_\theta$. This stress condition can be defined as a passive loading condition. In this paper, the equations for a passive loading condition will be shown.

Figure 1 shows a borehole of radius a in an infinite soil mass. The borehole is subjected to an internal pressure, p_i, which simulates a pressurized grouting and initial in-situ isotropic stress, σ_0^∞. For the elastic region, $r \geq b$, the radial and tangential stresses can be derived by the Kirsh solution as follows:

$$\sigma_r = \sigma_0^\infty\left(1-\frac{a^2}{r^2}\right)+p_i\left(\frac{a^2}{r^2}\right) \quad (1)$$

$$\sigma_\theta = \sigma_0^\infty\left(1+\frac{a^2}{r^2}\right)-p_i\left(\frac{a^2}{r^2}\right) \quad (2)$$

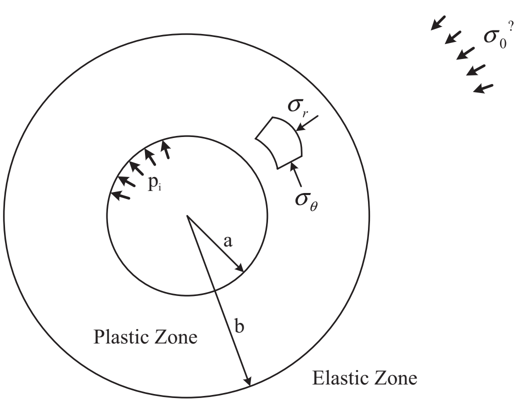

Figure 1. Elastic and plastic regions.

For a passive loading condition, the radial and tangential stresses in the plastic region ($a \leq r \leq b$) can be obtained as follows:

$$\sigma_r = \left(p_i+\frac{\sigma_c}{k-1}\right)\left(\frac{r}{a}\right)^{\frac{1}{k}-1}-\frac{\sigma_c}{k-1} \quad (3)$$

$$\sigma_\theta = -\frac{1}{k}\sigma_c+\frac{1}{k}\left[\left(p_i+\frac{\sigma_c}{k-1}\right)\left(\frac{r}{a}\right)^{\frac{1}{k}-1}-\frac{\sigma_c}{k-1}\right] \quad (4)$$

where $k = \tan^2\left(45+\frac{\phi}{2}\right)$; and

$$\sigma_c = 2c\tan\left(45+\frac{\phi}{2}\right) \quad (5)$$

The radius b for the passive loading condition can be obtained as follows:

$$b = a\left[\left(\frac{2\sigma_0^\infty-\frac{\sigma_c}{k}}{\frac{1}{k}+1}+\frac{\sigma_c}{k-1}\right)\frac{1}{p_i+\frac{\sigma_c}{k-1}}\right]^{\frac{1}{\frac{1}{k}-1}} \quad (6)$$

The radial displacement of a borehole can be obtained based on the elasto-plastic theory. The radial displacement at the borehole wall, $r = a$ under a passive loading condition can be expressed as Eq. (7):

$$u_r = \frac{1}{2G}a^{-\frac{1}{k_\psi}}\left[C(1-2\nu)\left(b^{\frac{1}{k_\psi}+1}-a^{\frac{1}{k_\psi}+1}\right)-D\left(b^{\frac{1}{k_\psi}-1}-a^{\frac{1}{k_\psi}-1}\right)\right]+u_{r(r=b)}\left(\frac{b}{a}\right)^{\frac{1}{k_\psi}} \quad (7)$$

$$C = \frac{(\sigma_h-\sigma_{r(r=b)})b^2-(\sigma_h-p_i)a^2}{b^2-a^2}; \quad \text{and } D = \frac{a^2b^2(a_{r(r=b)}-p_i)}{b^2-a^2}; \quad (8)$$

where G indicates the shear modulus, ν is the Poisson's ratio, k_ψ is the dilation angle.

Therefore, Eq. (7) makes it possible to estimate the radial displacement of a borehole caused by pressurized grouting and to evaluate the enlargement of the anchor body diameter.

2.2 *Permeation characteristics of pressurized grouting*

The permeation (penetrability) of cement grout is affected subject to the grain size distribution of base soils and cement, the concentration and viscosity of grout suspensions, the pore size of base soils, injection pressure, and the permeability of base soils. Moreover, the viscosity of grout suspension varies with time caused by chemical reactions that occur when the grout suspension moves through pores in the soil matrix. The increased viscosity of grout suspension causes a reduction in the permeability of grout through the soil matrix. Kim et al. (2009) studied the permeation characteristics of cement grout based on spherical coordinates. This paper utilized the solution proposed by Kim et al. (2009) to estimate the permeation distance of cement grout for the pressurized grouting of the grout anchor.

3 LABORATORY CHAMBER TESTS

3.1 *Experimental set-up*

Pilot-scale chamber tests were performed in order to investigate the effect of pressurized grouting on ground anchor. Figure 2 shows the chamber and apparatus set-up with full instrumentation. The chamber consisted of a cylindrical tank with an inside diameter of 600 mm and a height of 300 mm. Two earth pressure cells and two Linear Variable Differential Transducers (LVDTs) were installed to measure the earth pressure and displacement of the borehole caused by pressurized grouting, respectively. In addition, three pore water pressure transducers were mounted inside the borehole to measure the changes of the excess pore water pressure inside the grout with time. The grout injection equipment consisted of a packing device installed on the upper cap of the chamber and injection tank, being designed to discharge the inside grout to the outside soil by air pressure.

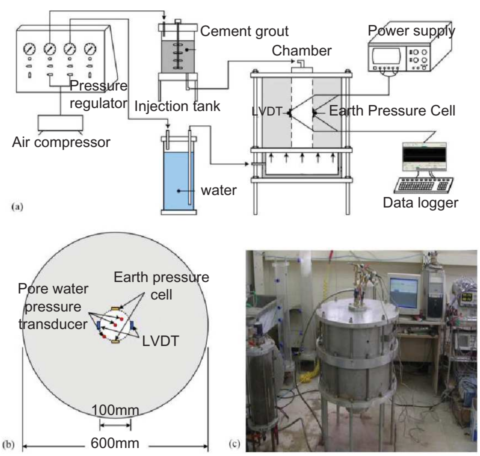

Figure 2. Experimental set-up for pilot-scale chamber test: (a) test set up with full instrumentation; (b) cross section of the chamber; and (c) photo of the chamber test in progress.

The soil samples for the chamber tests were collected from the areas of Jong-am Dong (Sample A), Jeon-nong Dong (Sample B), and Gong-duk Dong (Sample C) where the field tests were scheduled to be conducted. Soil properties of each sample were measured and summarized in Table 1. The injected grout suspension was prepared by mixing Portland cement with water to the ratio of 50%. The cement grout properties are summarized in Table 2. The viscosity change in grout suspension used in this study was measured by using a viscometer before injection. Figure 3 shows the viscosity of grout suspension with time and the relationship between grout viscosity and time is presented by the solid line. This curve is needed for the step wise numerical model shown in the next section (Kim et al. 2009).

The procedure for the chamber test was as follows. A soil specimen of 17.7 kN/m^3 unit weight was created by compaction, and LVDTs and earth pressure cells were installed to measure the expansion of the borehole and the pressure variation of the surrounding soil resulted from the grout injection. The drilling process was simulated by extracting a 100 mm diameter pipe after compaction which had been inserted during compaction. The vertical confining pressure of 88.5 kPa was applied to simulate an in-situ stress condition at a ground depth of 5.0 m. Subsequently, pressurized grouting was applied to three samples with the pressures of 196 kPa, 294 kPa, and 392 kPa, respectively.

3.2 *Penetration of cement grout into the soil*

The grout was injected for 1000 sec into the borehole. The amount of grout particles deposited in the soil matrix according to the distance from the injection hole was evaluated by using the step wise numerical model proposed by Kim et al. (2009) and is shown in Figure 4.

Even if the grout particles penetrate into the neighboring ground due to pressurized grouting, it does not necessarily confirm that the entire boundary in the neighboring ground is considered as the anchor body. Therefore, a certain criterion is required for the judgment of the boundary of an enlarged anchor body caused by the penetration of cement grout. For this purpose, the mixed soil-cement samples according to the mass of grout particles deposited per unit volume were prepared and uniaxial compression tests for each sample were

Table 1. Soil properties used in chamber test.

	Jong-am Dong (Sample A)	Jeon-nong Dong (Sample B)	Gong-duk Dong (Sample C)
Specific gravity, Gs	2.60	2.64	2.64
Friction angle, ϕ [deg]	32.74	34.41	31.67
Dilation angle, K [deg]	4.60	6.10	0.00
Cohesion, C [kPa]	20.47	25.57	25.51
Elastic modulus, E [MPa]	40.08	82.83	78.64
Poisson's ratio, kψ	0.400	0.394	0.407
Coefficient of permeability, k [cm/sec]	3.38×10^{-3}	2.21×10^{-4}	4.36×10^{-5}
Mean of pore radius lognormal distribution, m	–2.3055	–2.5859	–2.4487
Standard deviation of pore radius lognormal distribution, b	1.4097	1.2690	1.1071

Table 2. Cement grout properties used in chamber test.

Water-cement	50%
Initial concentration of grout	1.2 g/cm^3
Specific gravity of grout particle	3.0 g/cm^3
Average size of grout particle	0.011 mm

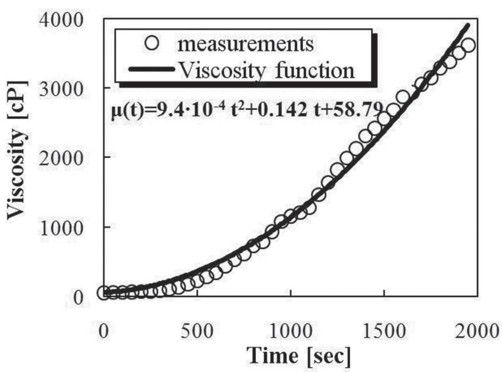

Figure 3. Change of grout viscosity with time.

carried out to evaluate the uniaxial compression strength. The results of uniaxial compression tests are shown in Figure 5. The criterion defined the mass of grout particles deposited per unit volume, $\sigma = 0.20$ g/cm^3, in which the sample shows a solid state, to judge the boundary of the anchor body of the ground anchor caused by the penetration of cement grout.

3.3 *Enlargement of anchor body diameter*

Table 3 shows the results of the enlargement of the anchor body diameter after 1000 sec pressurized grouting. The results were obtained from both the laboratory chamber tests and theoretical analyses.

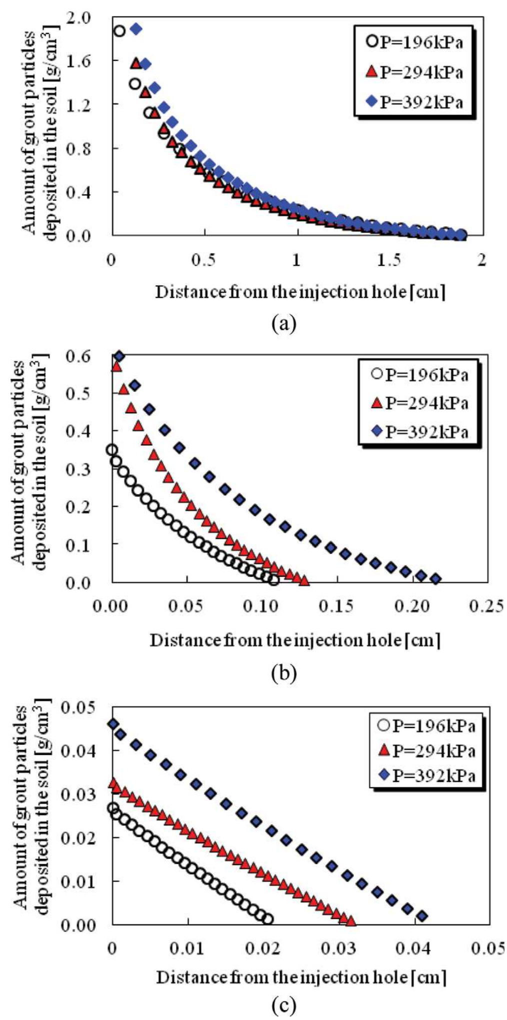

Figure 4. Amount of deposited particles with distance: (a) Jong-am Dong (sample A); (b) Jeon-nong Dong (sample B); and (c) Gong-duk Dong (sample C).

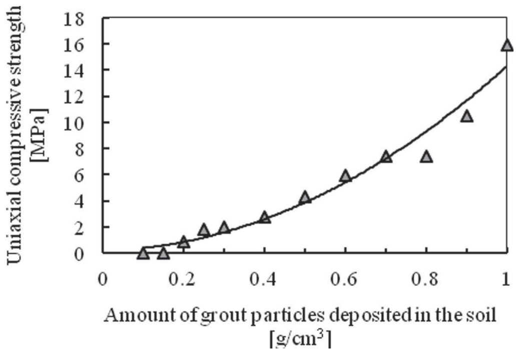

Figure 5. Result of uniaxial compression strength with amount of grout particles deposited.

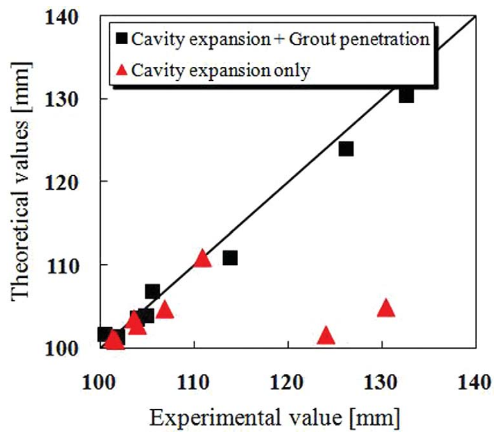

Figure 6. Comparison between test result and theoretical value of the enlargement of anchor body diameter.

Table 3. Results of enlargement of anchor body diameter.

	Results from theoretical analysis					Lab. test
	k [cm/sec]	Injection pressure [kPa]	Cavity expansion theory[1] [mm]	Grout penetration[2] [mm]	Cavity+ penetration[3] [mm]	Chamber test result[4)] [mm]
Sample A	3.38×10^{-3}	196	101.61	122.40	124.01	126.20
		294	104.91	125.50	130.41	132.41
Sample B	2.21×10^{-4}	196	100.94	100.65	101.59	100.48
		294	102.76	101.15	103.91	104.87
		392	104.72	102.10	106.82	105.54
Sample C	4.36×10^{-5}	196	101.27	–	101.27	101.87
		294	103.53	–	103.53	103.97
		294	102.76	–	110.80	113.87

1) Diameter obtained from cavity expansion theory only by using Equation (15) + 100 mm (borehole diameter); 2) Diameter obtained from grout penetration theory only by using step wise numerical analysis + 100 mm (borehole diameter); 3) Summation of cavity expansion and grout penetration ($^{(1)+2)}$ –100 mm (borehole diameter)); 4) Results from laboratory chamber tests.

The 4th, 5th, 6th and 7th columns indicate the final diameters of the anchor body evaluated from the cavity expansion theory (Eq. (7)) only, from the grout penetration theory proposed by Kim et al. (2009), from the summation of cavity expansion result and grout penetration result, and from the laboratory chamber tests, respectively. The comparison between the experimental test results (7th column) and the theoretical values (4th and 6th columns, respectively) is shown in Figure 6. The enlargement of the anchor body diameter estimated from the summation of the cavity expansion theory and grout penetration (6th column) matches well with that obtained from experiments. However, in the case where the ground has a larger permeability as noted in sample A, the evaluation of enlargement by adopting only the cavity expansion theory (4th column) can lead to underestimation. It can be concluded that the enlargement of the anchor body diameter caused by pressurized grouting must be estimated by combining the cavity expansion theory and the grout penetration theory, if the coefficient of permeability is larger than approximately 10^{-3} cm/sec.

4 FIELD TEST OF PRESSURIZED GROUTING GROUND ANCHOR

4.1 *Test method*

Field tests to measure the pullout resistance of the ground anchor, to identify the enlargement of the ground anchor body due to pressurized grouting were carried out 22 times in 5 phases as shown in Table 4. Field tests were conducted in the areas where the soil samples for laboratory chamber tests were collected. The physical properties were obtained through the in-situ and laboratory tests and their results are shown in Table 5. Herein, the SPT-N_{60} values representing each ground were shown after being calibrated based on 60% energy efficiency in a standard penetration test.

The procedure for the installation of the pressurized grouting ground anchor is shown in Figure 7, in which the assembled tendons were inserted into the inside of a casing after drilling with double casing, and a cement grout with a 50% water-cement ratio was then injected into the borehole through pressurized grouting. Pressure was applied on the head of the casing immediately after the casing was pulled up to the top of the bonded length. To measure the pullout resistance in an installed ground anchor, curing was applied for three days after construction and pullout tests were then performed. Since the purpose of this study is to compare the pullout resistances of pressurized grouting

Table 4. Field test results.

Site	Soil type	Average SPT-N60	Permeability [cm/sec]	Test case	Injection pressure [kPa]	Pullout resistance [kN]	Diameter of anchor body [mm]
Jong-am Dong (1st phase)*1	Silty sand	8	6.15×10^{-3}	A-1	100	445.1	168.1
				A-2	100	551.0	162.7
				A-3	100	572.0	163.1
				A-4	100	403.0	162.2
				A-5	–	297.0	143.8
Jeon-nong Dong (2nd phase)*2	Decomposed residual soil	21	1.37×10^{-4}	B-1	–	325.7	156.0
				B-2	220	386.5	164.0
				B-3	250	447.9	165.6
				B-4	250	470.8	164.0
Gong-duk Dong (3th phase)*2	Decomposed residual soil	66	1.20×10^{-4}	C-1	–	503.7	140.3
				C-2	196	470.4	142.3
				C-3	157	477.3	141.6
Ga-jwa Dong 1 (4th phase)*2	Decomposed residual soil	15	5.27×10^{-4}	D-1	–	170.4	–
				D-2	–	176.5	136.1
				D-3	196	302.1	–
				D-4	294	272.6	143.2
Ga-jwa Dong 2 (5th phase)*2	Decomposed residual soil	15	5.27×10^{-4}	D-5	220	238.8	–
				D-6	250	103.9	–
				D-7	230	405.0	–
				D-8	200	114.2	–
				D-9	280	394.6	–
				D-10	230	207.7	–

*1) l = 6 m ; *2) l = 5 m.

Table 5. Properties of field soil.

	Jong-am Dong (Sample A-F)	Jeon-nong Dong (Sample B-F)	Gong-duk Dong (Sample C-F)	Ga-jwa Dong (Sample D-F)
SPT-N60 value	8	21	66	15
Friction angle, ϕ [deg]	32.74	34.41	32.49	27.84
Cohesion, C [kPa]	20.47	25.57	25.51	4.90
Elastic modulus, E [MPa]	40.08	82.83	87.64	–
Poisson's ratio, kψ	0.4000	0.394	0.407	–
Coefficient of permeability, k [cm/sec]	6.15×10^{-3}	1.37×10^{-4}	1.20×10^{-4}	5.27×10^{-4}

Figure 7. Procedure for installation of pressurized grouting ground anchor: (a) drilling with double casing; (b) gravitational grouting; (c) insert tendons into the borehole; and (d) pressurized grouting.

with those of non-pressurized grouting and at the same time to evaluate the decrease in pullout resistance caused by the group effect, the ultimate pullout resistance of the ground anchor is defined as the maximum load at which the pullout displacement occurs continuously with no increase in the load. After the pullout test, the anchor body was dug out and investigated to measure the enlarged diameter of the anchor body.

4.2 *Effect of the pressurized grouting on ground anchor*

The field ground characteristics, grout injection pressure, ultimate pullout resistance and enlarged diameter of the anchor body obtained from a series of field tests are summarized in Table 4. In the case where pressurized grouting is performed, other than the case of non-pressurized grouting, the ultimate pullout resistance was found to increase by 1.66 times for silty sand and 1.47 times for decomposed residual soil ($N_{60} < 50$) on average, which proved that the injection of pressurized grouting is beneficial to raise the ultimate pullout resistance of a ground anchor.

Figure 8 shows the relationships between (a) pullout resistance vs SPT-N_{60}; (b) pullout resistance vs permeability; (c) diameter of anchor body vs SPT-N_{60}; and the field test result vs theoretical value. Herein, the ratio of pullout resistance means the ratio of pullout resistance of the pressurized grouting ground anchor to

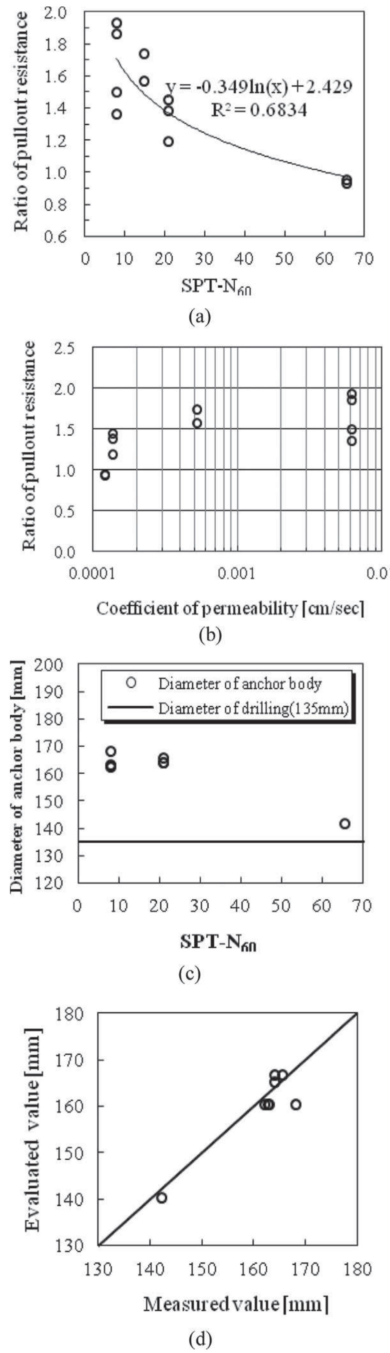

Figure 8. Field test results: (a) effect of pressurized grouting on pullout resistance according to SPT-N_{60} value; (b) effect of pressurized grouting on pullout resistance according to permeability; (c) enlargement of anchor body diameter according to SPT-N_{60} value; and (d) comparison of the enlargement of anchor body diameter between test result and theoretical value.

that of the non-pressurized ground anchor. When the pressurization was applied as can be seen in Figure 8(a) in comparison with non-pressurization, the field test results demonstrated that the ultimate pullout resistance for the case of decomposed residual soil whose SPT-N_{60} value was below 50 is increased by 1.19–1.74 times. However, the value for decomposed residual soil with an SPT-N_{60} value of more than 50 is increased by 0.93–0.95 times with little expectation of increasing pullout resistance due to pressurized grouting. As shown in Figure 8(b), it was found that a larger permeability in the ground corresponded to a higher effect in pullout resistance due to pressurized grouting. It was identified that the diameter of the ground anchor body in the case of performed pressurized grouting, exhibited a diameter larger than the drilled diameter as shown in Figure 8(c) when the ground has low SPT-N_{60} values. The enlargement of anchor body diameters estimated theoretically from the combination of the cavity expansion theory and the grout penetration theory matched reasonably well with the results obtained from field tests as shown in Figure 8(d).

5 CONCLUSIONS

The results of this study can be summarized as follows:

1. It was found that the grout penetration theory should be considered along with the cavity expansion theory in evaluating the enlargement of the anchor body diameter caused by pressurized grouting, if the permeability of the ground is larger than 10^{-3} cm/sec.
2. When the pressurization is applied to the compression anchor, the ultimate pullout resistance for the case of decomposed residual soil whose SPT-N_{60} value is below 50 should be increased by 1.19–1.74 times. However, the value for decomposed residual soil with an SPT-N_{60} value of more than 50 should be increased by 0.93–0.95 times with little expectation of increasing pullout resistance due to pressurized grouting. In addition, it is found that a larger permeability in the ground corresponds to a higher effect in pullout resistance due to pressurized grouting.

REFERENCES

Hobst, I.L. & Zajic, I.J. 1983. Anchoring in rock and soil. Amsterdam: 2nd Ed., Elsevier Scientific Publishers.

Kim, J.S., Lee, I.M., Jang, J.H., and Choi, H.S. 2009. Groutability of cement-based grout with consideration of viscosity and filtration phenomenon. *International Journal for Numerical and Analytical Methods in Geomechanics* 33(16): 1771–1797.

Kleyner, I.M., Krizek, R.J., and Pepper, S.F. 1993. Influence of grout pressure on capacity of bore-injected piles and anchors. *Proc., of the International Conference on Grouting in Rock and Concrete*, Salzburg, Austria: 159–165.

Yin, J.H., Su, L.J., Cheung, R.W.M., Shiu, Y.K., and Tang, C. 2008. The influence of grouting pressure on the pullout resistance of soil nail in compacted completely decomposed granite fill. *Geotechnique* 59(2): 103–113.

Yu, H.S. & Houlsby, G.T. 1991. Finite cavity expansion in dilatants soils: loading analysis. *Geotechnique* 41(2): 173–183.